Smart Structures and Systems, *Vol. 20, No. 1 (2017) 75-83*
DOI: https://doi.org/10.12989/sss.2017.20.1.075

Crack detection study for hydraulic concrete using PPP-BOTDA

Xiaofei Huang[†1,2,3], Meng Yang[*†1,2,3], Longlong Feng[†4], Hao Gu[1,2,3], Huaizhi Su[1,2,3], Xinbo Cui[5] and Wenhan Cao[1,2,3]

[1]*State Key Laboratory of Hydrology-Water Resources and Hydraulic Engineering, Hohai University, Nanjing 210098, China*
[2]*College of Water Conservancy and Hydropower Engineering, Hohai University, Nanjing 210098, China*
[3]*National Engineering Research Center of Water Resources Efficient Utilization and Engineering Safety, Nanjing 210098, China*
[4]*Gansu Middle East Construction Management Consulting Group, Lanzhou 730030, China*
[5]*Information Center of land and resources in binzhou city, Binzhou, China*

(Received May 12, 2016, Revised June 10, 2017, Accepted June 14, 2017)

Abstract. Effectively monitoring the concrete cracks is an urgent question to be solved in the structural safety monitoring while cracks in hydraulic concrete structures are ubiquitous. In this paper, two experiments are designed based on the measuring principle of Pulse-Pre pump Brillouin Optical Time Domain Analysis (PPP-BOTDA) utilizing Brillouin optical fiber sensor to monitor concrete cracks. More specifically, "V" shaped optical fiber sensor is proposed to determine the position of the initial crack and the experiment illustrates that the concrete crack position can be located by the mutation position of optical fiber strain. Further, Brillouin distributed optical fiber sensor and preinstall cracks are set at different angles and loads until the optical fiber is fractured. Through the monitoring data, it can be concluded that the variation law of optical fiber strain can basically reflect the propagation trend of the cracks in hydraulic concrete structures.

Keywords: concrete cracks; safety monitoring; Brillouin distributed optical fiber sensor

1. Introduction

Concrete has been widely used in all kinds of large-scale projects for its strong durability and high compressive strength. However, the tensile strength of concrete is low and the crack resistance is poor, especially in the large volume of concrete structures, the existence of cracks is very common (Pan *et al*. 2002, Su *et al*. 2013, Yang *et al*. 2015a). The common crack monitoring method is mainly through the laying of sensors, such as resistance strain gauge, differential resistance instrument and magnetoelastic torque sensor (Garus *et al*. 1995, Galindez-Jamioy *et al*. 2012, Yang *et al*. 2015b, Chen *et al*. 2016). This kind of point sensors can realize on-line real-time monitoring and quantitative detection, which provides a certain guarantee for the construction and safe operation of structures, while it also has its own shortcomings, such as the small monitoring scope, easy to be influenced by the space magnetic field and the poor durability (Lee *et al*. 2010, Su *et al*. 2014, François *et al*. 2015). In recent years, with the progress of science and technology, the optical fiber sensors developed rapidly. Optical fiber sensors have very good prospects, which are with the advantage of high accuracy, high sensitivity, relatively small volume and strong anti-electromagnetic interference ability (Goh *et al*. 2003, Liu *et al*. 2016). Compared with the conventional point sensors, optical fiber distributed sensors can consecutively obtain information on the distribution of area measurement. Optical fiber monitoring is mainly utilizing three kinds of light scattering occurred in optical fiber transmission, which are Rayleigh scattering, Raman scattering and Brillouin scattering (Kim *et al*. 2002, Minardo *et al*. 2009). At present, the research for Rayleigh scattering and Raman scattering has been relatively mature, instead, for Brillouin scattering, the research began later. Nevertheless, the accuracy, spatially resolved rate and distance measurement range of Brillouin scattering are better than others in structural monitoring, and can simultaneously measure strain and temperature (Falciai *et al*. 2005, Gogolla *et al*. 1997, Suh *et al*. 2008). Therefore, in this paper, BOTDA is utilized as a new monitoring method, which is applied to the monitoring of structural cracks.

With the continuous development of the optical fiber technology, many scholars have made some contribution to the Brillouin scattering optical fiber monitoring. Kurashima and Horiguchi established the Brillouin optical time domain reflectometry system and BOTDA system (Kurashima *et al*. 1997, Kurashima *et al*. 1993, Horiguchi *et al*. 1990, Horiguchi *et al*. 1989, Zhu *et al*. 2010); Kobyakov carried out an experiment on the strain and temperature through stimulated Brillouin scattering of the common fibers. The experimental results illustrated that utilizing Brillouin optical fiber monitoring technology for structure monitoring was with high precision (Kobyakov *et al*. 2010, Bao *et al*. 2016). In 1999, Geinitz utilized the optical fiber with the length of 12 km for test in order to compensate the system error, moreover the precision of the experiment was improved (Geinitz *et al*. 2011); Zornoza proposed to change the code of input pumping light, and its accuracy and

∗Corresponding author, Ph.D.
E-mail: ymym_059@126.com
† Contribute equally to the work

ISSN: 1738-1584 (Print), 1738-1991 (Online)

sensitivity were improved (Zornoza *et al*. 2012); In 2011, Galindez developed the improvement algorithm of data processing, so as to realize the dynamic measurement based on BOTDA (Galindez *et al*. 2011). Deqiao Li (2011) apply BOTDA to monitor the bending deformation of oil and gas pipeline. The strain distribution in the deformed area is obtained by the model test which provides a distributed strain monitoring method for practical engineering. Chaochao Xie (2013) analyze the variation of the concrete beam under the load by the variation of optical fiber strain which preliminarily realize the crack monitoring using BOTDA. Brillouin optical fiber sensing technology has obvious advantages in the monitoring of large structures with long distance, high precision, stable test performance and so on. Nevertheless, when using Brillouin scattering measurements to monitor strain, some problems still exist, such as monitoring system of low spatial resolution, the larger measurement error and the low sensitivity of crack monitoring (Soto *et al*. 2013, Kagimoto *et al*. 2015).Therefore, further research on these issues is needed in order to improve the accuracy of strain monitoring in the real project.

At present, the layout of fiber optic sensors to capture the location of cracks is simple which result in the low sensing ability of optical fiber sensor and the accurate judgment of the initial crack location. This paper proposes a continuous "V" shape using optical fiber sensor. Three point bending loading was performed by universal testing machine and NBX-6050A optical nano meter was used to measure strain. Determine the state of concrete cracking according to the measurement of optical fiber strain distribution and change. This paper also puts forward the skew sensor based on Brillouin optical time domain analysis to monitor the variation of the width and the randomness of the crack. The performance when the fiber optic sensor and the crack are at different angles is studied by simulation test which provide the corresponding reference of determining the crack width and direction in to the future projects.

2. Application of BOTDA in structural crack monitoring

2.1 Brillouin optical fiber sensing theory

Under normal circumstances, the scattering of light will occur in the process of transmission in the fiber media. The distributed optical fiber sensing system mainly includes 3 kinds of scattering, Raman scattering, Rayleigh scattering and Brillouin scattering (Brown *et al*. 2005). Spectrum distribution can be seen in Fig. 1.

Brillouin scattering is first discovered by Brillouin Leon, which is produced by the interaction of optical photons and acoustic phonons (Bao *et al*. 1999, Nikles *et al*. 1997). The common optical fiber is mainly made of silica. Silicon is with the property of electrostriction, therefore the fiber also has the property of electrostriction. When the power of pump light become relative large in optical fiber transmission, the fiber refraction rate will change, resulting in electrostriction cause in fiber medium, which makes a large portion of the incident light transform to the backward scattering light in the fiber. Consequently, stimulated Brillouin scattering is formed (Pinto *et al*. 2012, Kellie *et al*. 2005). The process of stimulated Brillouin scattering can be seen in Fig. 2.

2.2 Influence of cracks on Brillouin optical fiber sensors

The distributed optical fiber sensors based on BOTDA has been widely used in the field of structural monitoring. However, at present, the BOTDA research is mainly based on experiments, which is difficult to capture the location of the cracks, and how the cracks will develop also need to be focused. In view of this, this paper focuses on the use of "V" shaped fiber optic sensor to monitor the initial crack of three-point bending concrete beam. Then the fiber optic sensors and the preinstalled cracks of concrete beams are arranged in different angles in order to study the monitoring performance of the sensors, which provides a certain basis for monitoring cracks in the actual project.

As the matter of fact, the crack position in hydraulic concrete structure is random and uncertainty. Therefore, the relationship between crack width, layout of the optical fiber and calibration length will be derived as follows.

Assume that only a crack passes through the optical fiber, which can be seen in Fig. 3.

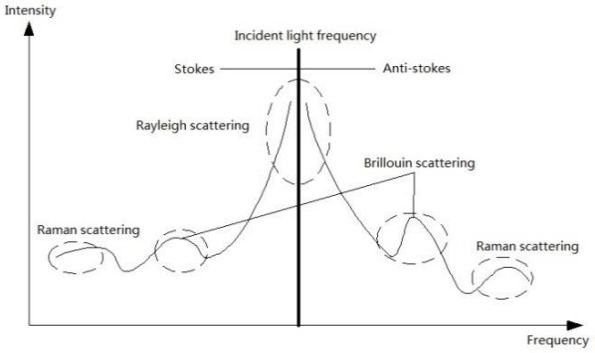

Fig. 1 Spectrum distribution

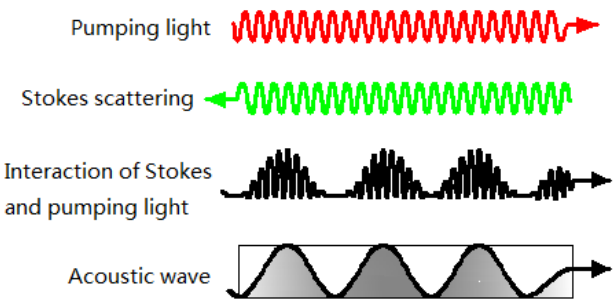

Fig. 2 The process of stimulated Brillouin scattering

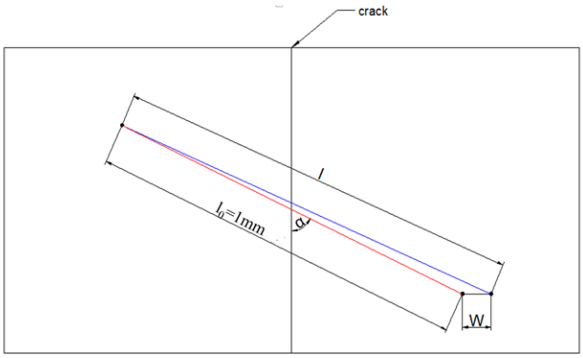

Fig. 3 Layout of the optical fiber

In Fig. 3, l_0 is calibration length, which is the fix distance of two ends. And, the length of the l_0 is 1mm. l is the length of optical fiber after crack propagation; w is the width of the crack; α is the angle between the optical fiber and the crack. $\alpha \in [0, 90^\circ]$

The two assumptions are made before deriving the relationship of those variables:

(1) The deformation of the optical fiber is consistent with the deformation of the test structure.

(2) The fiber and the test structure paste firmly, and will not generate relative sliding.

The definition of strain in mechanics can be rewritten to

$$\varepsilon = \frac{l - l_0}{l_0} = \frac{\sqrt{l_0^2 + w^2 - 2l_0 w\cos(90^\circ + \alpha)} - l_0}{l_0} = \sqrt{\left(\frac{w}{l_0}\right)^2 + 2\frac{w}{l_0}\sin\alpha + 1} - 1 \quad (1)$$

In Eq. (1), it is known that the strain of optical fiber is correlative with the crack width, calibration length of optical fiber and the angle between the optical fiber and the crack. The relation curves between the strain of optical fiber sensors and the crack width of the test structure can be drawn utilizing Eq. (1), as shown in Fig. 4.

2.3 The relationship between Brillouin frequency shift and strain

The change of the strain in the optical fiber result in the change of the refractive index and the sound velocity, so the Brillouin frequency shift changes. In the case of single-mode optical fiber, Brillouin frequency shift can be expressed by the Eq. (2).

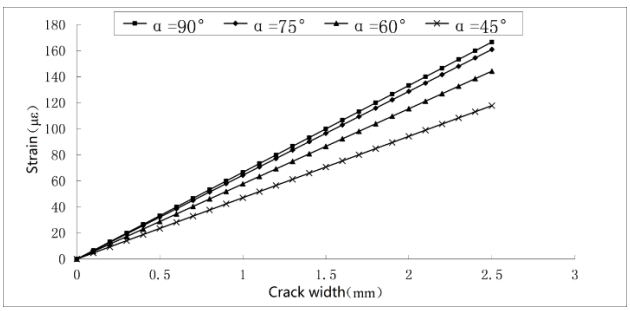

Fig. 4 The variation relation between the strain and crack width

$$\upsilon_B = \frac{2nv_A}{\lambda_R} \quad (2)$$

In this equation, υ_B is Brillouin frequency shift; n is refractive index of optical fiber; λ_R is wavelength of incident wave; υ_A is acoustic wave velocity.

In addition, the frequency of incident wave and scattering angle have great influence on the Brillouin frequency shift, and the corresponding relation is shown in the Eq. (3).

$$\upsilon_B = \upsilon_0 - \upsilon_s = \upsilon_{as} - \upsilon_0 = 2\upsilon_0 nv_A \sin(\theta/2)/c = 2nv_A/\lambda_0 \quad (3)$$

υ_0 ,υ_{as},υ_s represent the frequency of incident light, stokes and anti-stokes respectively. c is velocity of light in vacuum. λ_0 is the wavelength of incident light in vacuum.

Normally, the sound velocity is only related to the inherent properties of the material, such as Poisson's ratio μ, elastic modulus E, density ρ and so on.

$$v_A = \sqrt{\frac{(1-\mu)E}{(1+\mu)(1-2\mu)\rho}} \quad (4)$$

These inherent properties of optical fibers can be considered as a function of strain and temperature which can be expressed as $E(\varepsilon,T)$、$\mu(\varepsilon,T)$、$\rho(\varepsilon,T)$、$n(\varepsilon,T)$. Combine Eqs. (3) and (4) to obtain the relationship between Brillouin frequency shift, strain and temperature which is showed in Eq. (5).

$$\upsilon_B = \frac{2\upsilon_0}{c} n(\varepsilon,T)\sqrt{\frac{(1-\mu(\varepsilon,T))E(\varepsilon,T)}{(1+\mu(\varepsilon,T))(1-\mu(\varepsilon,T))\rho(\varepsilon,T)}} \quad (5)$$

Ignore the influence of temperature change and the relationship between Brillouin frequency shift and strain can be obtained.

$$\upsilon_B(\varepsilon,T_r) = \frac{2\upsilon_0}{c} n(\varepsilon,T_r)\sqrt{\frac{(1-\mu(\varepsilon,T_r))E(\varepsilon,T_r)}{(1+\mu(\varepsilon,T_r))(1-\mu(\varepsilon,T_r))\rho(\varepsilon,T_r)}} \quad (6)$$

Because the strain of optical fiber belongs to the range of small deformation, make Taylor extension to

Eq. (6) when ε=0. The relationship between Brillouin frequency shift and strain can be obtained by taking the constant term and the first term as shown in Eq. (7).

$$\upsilon_B(\varepsilon,T_r) = \upsilon_B(0,T_r)\left(1 + (\Delta n_\varepsilon + \Delta E_\varepsilon + \Delta\mu_\varepsilon + \Delta\rho_\varepsilon)\varepsilon\right) + o(\varepsilon^2) \quad (7)$$

The expression of the coefficients in Eq. (7) are as follows.

$$\begin{cases} \Delta n_\varepsilon = \dfrac{n_\varepsilon}{n(0,T_r)} \\ \Delta E_\varepsilon = \dfrac{E_\varepsilon}{2E(0,T_r)} \\ \Delta\rho_\varepsilon = \dfrac{-\rho_\varepsilon}{2\rho(0,T_r)} \\ \Delta\mu_\varepsilon = \dfrac{\mu_\varepsilon\mu(0,T_r)\left[2-\mu(0,T_r)\right]}{\left[1-\mu^2(0,T_r)\right]\left[1-2\mu(0,T_r)\right]} \end{cases} \quad (8)$$

n_ε, E_ε, ρ_ε, $\mu_\varepsilon$are strain coefficients of refractive index, elastic modulus, density and Poisson's ratio respectively. Simplify Eq. (7) to obtain Eq. (9).

$$\upsilon_B(\varepsilon) = \upsilon_B(0, T_r)(1 + C_\varepsilon \varepsilon) \tag{9}$$

In Eq. (9), ε is optical fiber strain and C_ε is strain scale factor. The relationship between Brillouin frequency shift and strain is linear according to Eq. (9) since the strain of optical fiber belongs to the range of small deformation

3. Experiment on the "V" shaped optical fiber sensing for the process of crack initiation

3.1 Experimental design

Under usual circumstances, hydraulic concrete structures will generate cracks under pressure, temperature and other loads, while crack position is random and uncertainty and difficult to capture. In view of this, optical fiber sensors will be laid into a continuous "V" shape, pasted on the bottom of the concrete beam in order to study perception ability and sensitivity of sensing initial cracks.

In this experiment the concrete mark is C30 and water-cement ratio is 0.45. The concrete pouring mold size is 150 mm * 150 mm * 550 mm (high x width x length). In order to load sustainably without brittle fracture, two tensile reinforcements are buried in the bottom of the mold. Its diameter is Φ 8 mm, as shown in Fig. 5.

In this experiment, the main instruments are: NBX-6050A optical nano meter, as shown in Fig. 6; SMF-28e common single-mode fiber and electronic universal testing machine, the model is RE-8060, and the maximum load can reach 600 kN. The accuracy is about ±7.5 με using our technique, which is better than other techniques with about ±10 με.

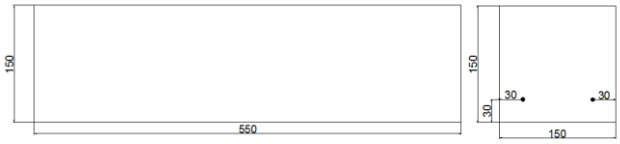

Fig. 5 Layout of tensile reinforcements (unit: mm)

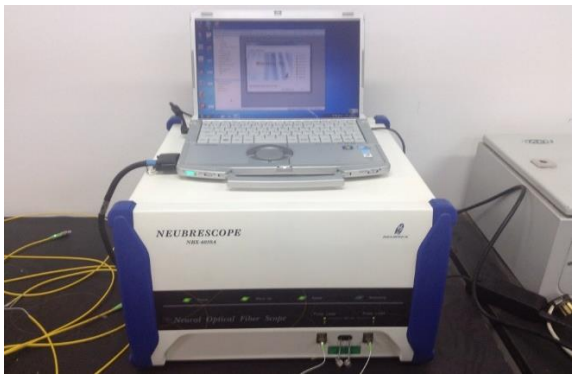

Fig. 6 NBX-6050A optical nano meter

3.2 Layout of the sensors

In this experiment, the fiber is pasted at the bottom of the concrete mold, utilizing epoxy structure AB glue to adhere. Optical fiber sensor is set to continuous "V" shape, pasted on tension side of the concrete mold. Record half "V" as a section, the optical fiber sensor is divided into 8 sections, as can be seen in Fig. 7(a). When the concrete beam cracks, the strain of the optical fiber sensor is changed, and the crack location is determined by the mutation of strain. The "V" shape optical fiber sensor can basically determine the location of the initial crack. The length of each section is approximately 130 mm, and each section makes about 15-degree angle with the cross-section of the mold. In order to ensure the turning of the fiber will not generate larger initial strain, an elliptical ring junction is laying at the turning. Utilize plastic bags to protect the optical fiber connectors, in case contamination. The layout can be seen in Fig. 7(b).

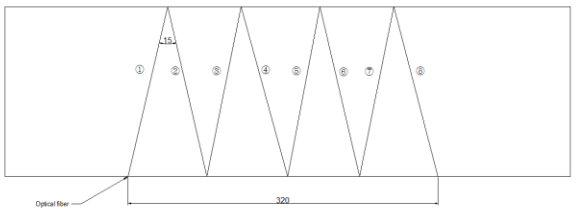

(a)

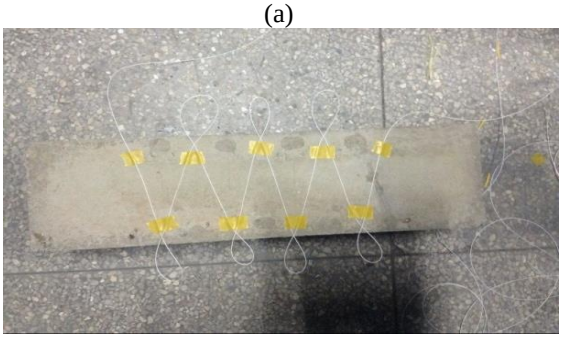

(b)

Fig. 7(a) Schematic diagram of "V" shaped optical fiber (degree unit: °; length unit: mm) and (b) The layout of "V" shaped optical fiber

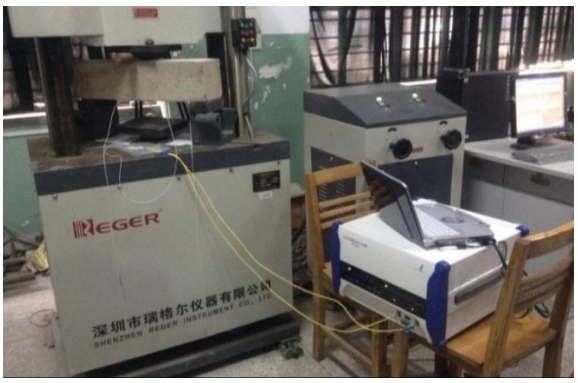

Fig. 8 The experimental site

Load with three-point bending mode of electronic universal testing machine. At this time, the concrete mid-span section is mainly under the axial tensile strain, and shear strain can be ignored. Therefore, the optical fiber is tilted in the region. When the concrete generates cracks, the strain will mutate. The experimental site can be seen in Fig. 8.

3.3 The experimental results discussion

In order to ensure the accuracy of the measurement, the parameter setting of the NBX-6050A optical nano meter should be firstly set. The PPP-BOTDA spatial resolution is set to 0.05 m and the sampling interval is 0.05 m.

Loading mode is displacement control and the fiber optic strain distribution before loading is shown as Fig. 9. When the concrete load reached 22.74 kN (control displacement was 0.6 mm), the initial micro crack generated (denoted as Crack I) which passed through Fiber④. At this time, the fiber strain distribution of each section is shown in Fig. 10.

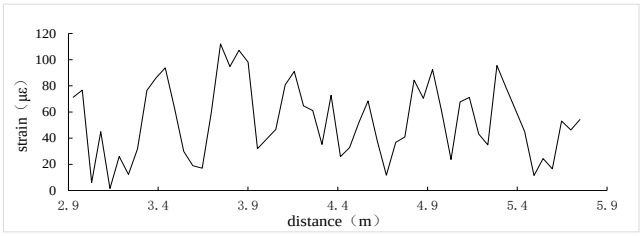

Fig. 9 The fiber optic strain distribution before loading

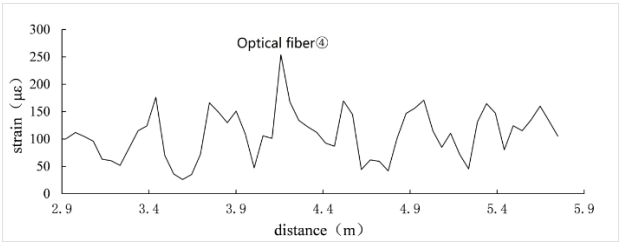

Fig. 10 The fiber optic strain distribution when the load reaches 22.74 kN

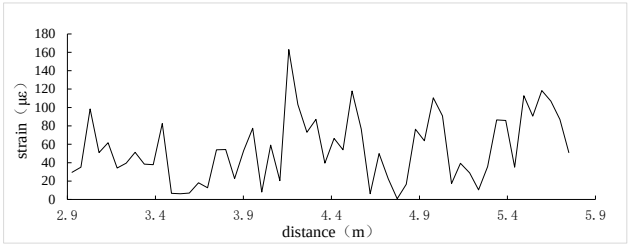

Fig. 11 The differential curve of the optical fiber strain between the loading of 22.74 kN and before loading

Fig. 12 The position of Crack I

Compared Fig. 9, Fig. 10 with Fig. 11, the strain of optical fiber④ mutated when the load was 22.74 kN. Actually a micro crack was produced at the bottom of the concrete mold, which was extended on the lateral face, as shown in Fig. 12. Furthermore, the crack passed through optical fiber④ which is consistent with the mutation of optical fiber④.

With the increasing of the control displacement and the load reaching 31.82 kN, a new micro crack (denoted as Crack II) was generated, and the crack passed through optical fiber⑦. The strain distribution of each optical fiber can be seen in Fig. 13. When the load reached 40.16 kN, the control displacement increased to 1.5 mm. At this time, a new crack was produced near optical fiber② (denoted as Crack III). Furthermore, Crack III firstly passed through optical fiber②, then through optical fiber① with the increasing load. The strain distribution after the generation of Crack III can be seen in Fig. 14.

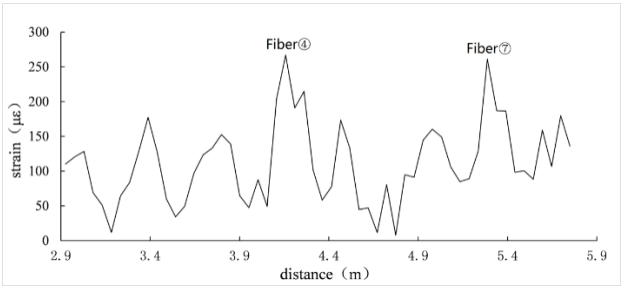

Fig. 13 The fiber optic strain distribution when the control displacement is 0.8 mm

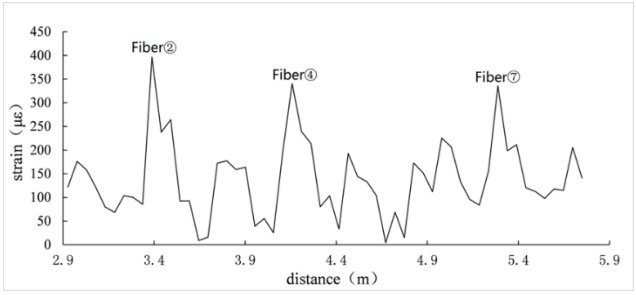

Fig. 14 The fiber optic strain distribution when the control displacement is 1.5 mm

Table 1 Correlation information of the experiment before and after strain mutation

Crack numbering	Load level (kN)	Displacement Control (mm)	Fiber numbering passed though by a crack	The measurement of optical fiber strain		
				Before mutation (με)	After mutation (με)	Mutation rate
I	22.74	0.6	④	137.513	249.293	81.3%
II	31.82	0.8	⑦	163.119	261.345	60.2%
III	40.16	1.5	②	244.722	396.645	62.1%
III	59.72	2.0	①	186.002	343.822	84.9%

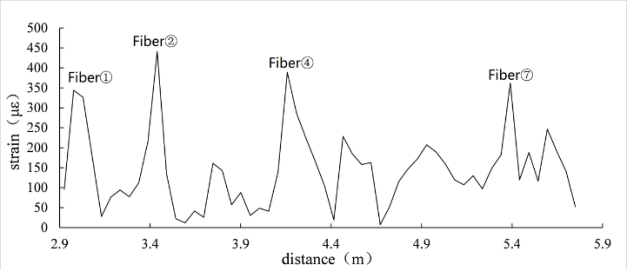

Fig. 15 The fiber optic strain distribution when the control displacement is 2.0 mm

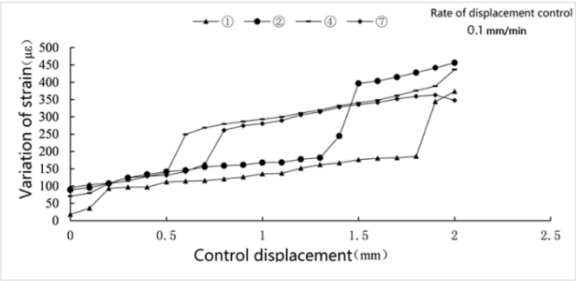

Fig. 16 The variation curve of maximum strain of optical fiber passed through by a crack

The strain distribution can be seen in Fig. 15 when the control displacement reached 2 mm and the load reached 46.68kN. Furthermore, it can be seen from Fig. 15 that①, ②, ④, ⑦ optical fiber all sensed cracks. The maximum strain value of the 4 optical fibers can be seen in Fig. 16.

In Figs. 9-11, Figs. 13-15, the 'distance' in the x-axis is the length of optical fiber. As Fig. 8 shows, the length of the optical fiber includes patch cables and the measuring section. So 2.9-5.9 m is the length of measuring section.

The variation curve of maximum strain for each optical fiber which is passed by cracks can be seen in Fig. 16. Therefore, load before and after strain mutation, strain of optical fiber and strain mutation values are listed in Table 1.

It can be seen from Table 1 that the strain of optical fiber will change under two adjacent loads. As the variation value is relative large, which illustrates the optical fiber strain mutates. Furthermore, the cross section of the concrete mold is mainly under the axial tensile strain and shear strain can be neglected. Therefore, it can be approximated considered that the crack is extended to the location where the optical fiber strain mutates. Through the observation of crack development, the conclusion is basically consistent with the result of optical fiber strain variation. In summary, "V" shaped optical fiber can realize the capture of the initial concrete crack position. Furthermore, oblique crossing optical fiber is utilized to monitor the crack development, the details are as follows.

4. The experiment on oblique crossing Brillouin optical fiber monitoring the widths of concrete cracks

4.1 Experimental design

From the analysis of Section 2.2 and on the basis of Chapter 3, set Brillouin distributed optical fiber sensors and preinstalled cracks at different angles. Through the variation law between optical fiber strain and the crack width under different angles, provide a certain reference for the real project.

The mold size, water-cement ratio, reinforcement and experimental equipments are completely consistent with those in the last experiment.

4.2 Layout of the sensors

The experiment is divided into four groups, and the optical fiber sensor and a preinstalled crack are set at an angle of 90°, 75°, 60° and 45° in each group respectively. Make attempt to set the optical fiber sensors in the middle position of the tensile region of the concrete mold. Set two fiber optic sensors symmetrically in case the optical fiber is spoiled. Optical fiber connectors are protected with plastic bags to prevent damage in the moving process. The schematic diagram of angle layout and the experiment site can be seen in Figs. 17 and 18 respectively.

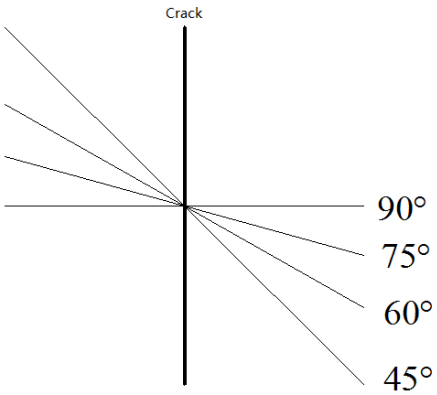

Fig. 17 The schematic diagram of angle layout

(a)

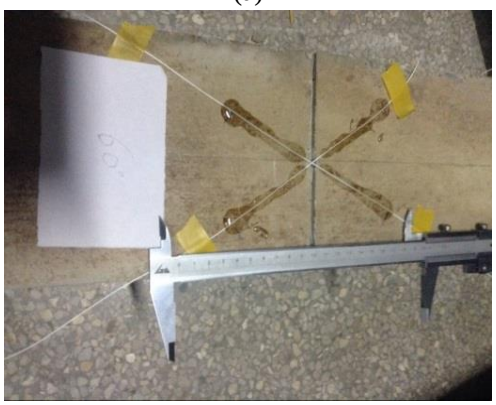

(b)

Fig. 18 (a) The experiment site of 45°optical fiber and The experiment site of 60°optical fiber

4.3 The experimental results discussion

In the four groups of experiments, as soon as the fiber optic sensor in each group was fractured, the universal testing machine stopped and the experiment was finished. The crack process of the concrete mold during the loading is demonstrated in Fig. 19.

During the experiment, the loading mode is displacement control. The displacement speed control of constant loading rate is 0.1 mm/min. In order to express the relationship between the two more intuitively, the changing relation between optical fiber strain and the crack widths at different angles is exhibited in Fig. 20.

Through the analysis of the experimental data, it can be concluded that optical fiber strain value increases with the expansion of the crack width in each group at the same angle. As the crack width is the same, the larger angle is, the larger optical fiber strain is. It can be seen from Fig.20 that at the beginning of loading, the load was relatively small, the change of crack width was small, but the variation of strain was relatively large, the relationship between the two was not obvious. When the control displacement reached 0.5 mm, the load was raising, at this time, the crack width at the bottom of the concrete mold increased obviously, optical fiber strain and crack width exhibited linear relationship.

Fig. 19 Cracking process of concrete mold during the experiment

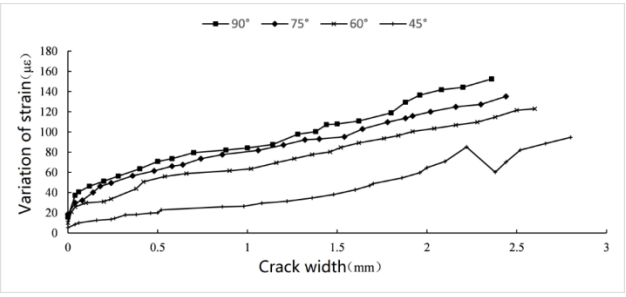

Fig. 20 The relationship between crack width and optical fiber strain at different angles

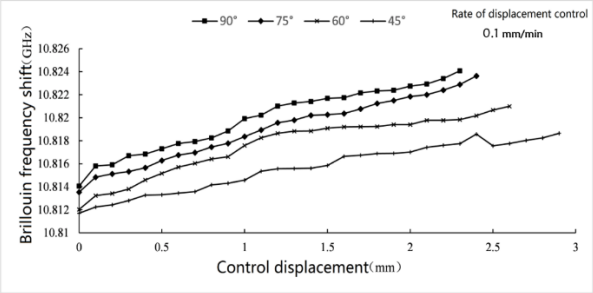

Fig. 21 Variation of Brillouin frequency shift at different angles during the loading

Compared to Fig. 4, under the premise of ignoring the error, the changing law of experimental results and theoretical curves of 90°, 75° and 60° is basically consistent, under the corresponding crack widths, the optical fiber strain values are relatively close. While the optical fiber strain value of 45° is smaller than the theoretical one, the reason maybe is that the epoxy structural to adhere optical fiber is not well solidified, result in certain sliding during the loading.

The optical fiber strain value of 45° declined sharply when the crack width was extended to about 2.22 mm, and then increased slowly. The reason is that: (1) the optical fiber sensor is generated a certain sliding on the surface of the concrete mold (2) the angle between the optical fiber and concrete crack is relative small under relative large load. When the load reach to a certain extent, a sliding occurs between fiber core and tight buffer, which results in the fiber stress redistribution, leading to the fluctuation of optical fiber strain. The actual monitoring results in Fig. 20 are unable to achieve complete agreement with theoretical data because of the uncontrollable factors. The results in Fig. 20 and Fig. 4 show small fluctuations while they are in accordance with the basic test assumptions and possible deviations. The small numerical differences do not affect the final consistent conclusions which shows the rationality and scientificalness of this experiment and mathematical model.

In order to describe the variation situation of Brillouin frequency shift, the variation of Brillouin frequency shift at different angles during the loading can be seen in Fig. 21.

It can be seen from Fig. 21 that the changing law of Brillouin frequency shift is consistent with the changing law of optical fiber strain during the loading, which is increasing with the raise of the load. The theoretical analysis to show why the changing law of Brillouin frequency shift is consistent with the one of optical fiber strain during the loading is explained in chapter 2.3. The measured data in Fig. 21 proves the relationship between Brillouin frequency shift and strain in Eq. (9).

In a word, when the preinstall cracks and optical fibers are arranged at different angles, at first load is relative small, and the width of crack is relative small. As a result, it is difficult to measure accurately utilizing the optical fiber sensor. When the crack is extended to a certain extent, crack width becomes larger, result in the increasing in the measurement of optical fiber strain, and the variation law between the two is gradually manifested. As a consequence, the change law of the optical fiber strain can basically reflect the propagation trend of the structural cracks.

5. Conclusions

In order to monitor the position where the initial concrete crack produces, "V" shape optical fiber is pasted at the bottom of the concrete mold. With the raise of the load, the strain of Brillouin optical fiber is also increasing. When a crack is generated, the corresponding optical fiber strain mutates. As a consequence, the crack position of the concrete mold can be located by the mutation position of optical fiber strain. In a word, the position of initial concrete cracks can be determined by utilizing "V" shaped optical fiber sensor.

From the experiment on oblique crossing optical fiber monitoring the widths of concrete cracks, it can be concluded that the optical fiber strain is increasing gradually with the propagation of cracks during the loading. Moreover, the two is on the whole exhibited linear variation. From the experimental data, under the other same conditions, the larger the angle of optical fiber and crack is, the greater the optical fiber strain is measured. In summary, the variation law of the optical fiber strain can basically reflect the propagation trend of the cracks in concrete structures.

The layout of the optical fiber may be very complex in mass concrete structures to obtain precise location of cracks. Moreover, improving the multiplexing capability of optical fiber in practical application and reducing the data receiving terminal to simplify the process of data processing is also a difficult research topic.

Acknowledgments

This research has been partially supported by the National Key Research and Development Program of China (SN:2016YFC0401601), National Natural Science Foundation of China (SN: 51579083, 51379068, 51479054, 41323001, 51139001, 51279052, 51579086, 51579085), Open Foundation of State Key Laboratory of Hydrology-Water Resources and Hydraulic Engineering (SN: 20145027612, 20165042112), , the Fundamental Research Funds for the Central Universities (Grant No. 2016B04114, 2015B25414, 2014B37114, 2014B37414, 2015B25414, 2015B20714, 2014B1605336), Jiangsu Natural Science Foundation (Grant Nos. BK20140039), the Doctoral Program of Higher Education of China (SN: 20130094110010), Project Funded by the Priority Academic Program Development of Jiangsu Higher Education Institutions (Grant No. YS11001), Jiangsu Basic Research Program (Grant Nos. BK20160872).

References

Bao, X., Brown, A., Demerchant, M. et al. (1999), "Characterization of the Brillouin-loss spectrum of single-mode fibers by use of very short (10-ns) pulses", *Opt. Lett.*, **24**(8), 510-512.

Bao, Y., Tang, F., Chen, Y., Meng, W., Huang, Y. and Chen, G. (2016), "Concrete pavement monitoring with PPP-BOTDA distributed strain and crack sensors", *Smart Struct. Syst.*, **18**(3), 405-423.

Brown, A.W, Colpitts, B.G. and Brown, K. (2005), "Distributed sensor based on dark-pulse Brillouin scattering", *IEEE Photonics Technol. Lett.*, **17**(7), 1501-1503.

Chen, S.S., Fu, Z.Z., Wei, K.M. and Han, H.Q. (2016), "Seismic responses of high concrete face rockfill dams: A case study", *Water Sci. Eng.*, **9**(3), 195-204.

Falciai, R. and Trono, C. (2005), "Curved elastic beam with opposed fiber-Bragg gratings for measurement of large displacements with temperature compensation", *IEEE Sens. J.*, **5**(6), 1310-1314.

François, N. and Félix, D. (2015), "Describing failure in geomaterials using second-order work approach", *Water Sci. Eng.*, **8**(2), 89-95.

Galindez-Jamioy, C.A. and López-Higuera, J.M. (2012), "Brillouin distributed fber sensors: An overview and applications", *J. Sensors*, **61**(1), 276-283.

Galindez, C.A., Madruga, F.J. and Lopez-Higuera, J.M. (2011), "Efficient dynamic events discrimination technique for fiber distributed Brillouin sensors", *Opt. Express*, **19**(20), 18917-18926.

Garus, A. D, Krebber, K., and Hereth, R. (1995), "Distributed fiber optical sensors using Brillouin backscattering", *Proceedings of SPIE - The International Society for Optical Engineering*, 172-183.

Geinitz, E., Jetschke. S., Röpke, U. et al. (1999), "The influence of pulse amplification on distributed fibre-optic Brillouin sensing and a method to compensate for systematic errors", *Meas. Sci. Technol.*, **10**(2), 112-116.

Gogolla, T. and Krebber, K. (1997), "Fiber sensors for distributed temperature and strain measurements using Brillouin scattering and frequency-domain methods", *Proceedings of SPIE - The International Society for Optical Engineering*, 3105.

Goh, C.S., Mokhtar, M.R., Butler, S.A. et al. (2003), "Wavelength tuning of fiber Bragg gratings over 90 nm using a simple tuning package", *IEEE Photonics Technol. Lett.*, **15**(4), 557-559.

Horiguchi, T. and Tateda, M. (1989), "BOTDA-nondextructive measurment of single-mode optical fiber attenuation characteristics using Brillouin interaction: Theory", *J. Lightwave Technol.*, **7**(8), 1170-1176.

Horiguchi, T., Kurashima, T. and Tateda, M. (1990), "Nondestructive measurement of optical fiber tensile strain distribution based on Brillouin spectroscopy", *T. IEICE Japan*, **7**(3). 144-152.

Kagimoto, H., Yasuda, Y. and Kawamura, M. (2015), "Mechanisms of ASR surface cracking in a massive concrete cylinder", *Adv. Concrete Constr.*, **3**(1), 39-54.

Kellie, B., Anthony, W.B. and Bruce, G.C. (2005), "Characterization of optical fibers for optimization of a Brillouin scattering based fiber optic sensor", *Opt. Fiber Technol.*, **10**(11), 131-145.

Kim, S.H., Lee, J.J. and Kwon, I.B. (2002), "Structural monitoring of a bending beam using Brillouin distributed optical fiber sensors", *Smart Mater. Struct.*, **11**(3), 396-403(8).

Kobyakov, A., Sauer, M. and Chowdhury, D. (2010), "Stimulated Brillouin scattering in optical fibers", *Adv. Opt. Photonics*, **2**(1), 1-59.

Kurashima, T., Horiguchi, T., Izumita, H. et al. (1993), "Brillouin optical-fiber time domain reflectometry", *IEICE T. Commun.*, **76**(4), 382-390.

Kurashima, T., Tansks, K. and Butler, S.A. (1997), "Application of fiber optic distributed sensor for strain measurement in civil engineering", *SPIE*, **32**(41), 247-258.

Lee, J., Yun, C. and Yoon, D. (2010), "Technical design note: A structural corrosion-monitoring sensor based on a pair of prestrained fiber Bragg gratings", *Meas. Sci. Technol.*, **21**(1), 1-7.

Li, D. (2011), "Study on influence factors of pipeline bending deformation monitoring based on distributed optical fiber sensing technology", Zhongbei University.

Liu, S. and Bauer, E. (2016), "Preface for special section on long-term behavior of dams", *Water Sci. Eng.*, **9**(3), 173-174.

Minardo, A. and Bernini, R.Z.L. (2009), "A simple technique for reducing pump depletion in long-range distributed Brillouin fiber sensors", *IEEE Sen. J.*, **9**(6), 633-634.

Nikles, M., Thevenaz, L. and Robert, P.A. (1997), "Brillouin gain spectrum characterization in single-mode optical fibers", *IEEE/OSA J. Lightwave Technol.*, **15**(10), 1842-1851.

Pan, J.Z. (2002), "There are no dams without cracks in the world", *China Three Gorges construction*, **9**(4), 6-7.

Pinto, A.M.R. and Lopez-Amo, M. (2012), "Photonic crystal fibers for sensing applications", *J. Sensors*, **2012**(1), 276-283.

Soto, M. A, and Thévenaz, L. (2013), "Modeling and evaluating the performance of Brillouin distributed optical fiber sensors", *Opt. Express*, **21**(25), 31347.

Su, H.Z., Hu, J., Li, J.Y. and Wu, Z.R. (2013), "Deep stability evaluation of high-gravity dam under combining action of powerhouse and dam", *Int. J. Geomech.*, **13**(3), 257-272.

Su, H.Z., Li, J.Y., Cao, J.P. and Wen, Z. (2014), "Macro-comprehensive evaluation method of high rock slope stability in hydropower projects", *Stoch. Env. Res. Risk A.*, **28**(2), 213-224.

Suh, K. and Lee, C. (2008), "Autocorrection method for differential attenuation in a fiber-optic distributed-temperature sensor", *Opt. Lett.*, **33**(16), 1845-1847.

Xie, C. (2013), "Research on structural health monitoring based on distributed optical fiber sensor based on BOTDA", Harbin Institute of Technology.

Yang, M. and Liu, S. (2015), "Field tests and finite element modeling of a Prestressed Concrete Pipe pile-composite foundation", *J. Civil Eng. KSCE*, **7**(19), 2067-2074.

Yang, M., Su, H.Z. and Yan, X.Q. (2015), "Computation and analysis of high rocky slope safety in a water conservancy project", *Discrete Dyn. Nat. Soc.*, **197579**, 1-11.

Zhu, H.H., Yin, J.H., Dong, J.H. and Zhang, L. (2010), "Physical modelling of sliding failure of concrete gravity dam under overloading condition", *Geomech. Eng.*, **2**(2), 89-106.

Zornoza, A., Sagues, M. and Loayssa, A. (2012), "Self-heterodyne detection for SNR improvement and distributed phase-shift measurements in BOTDA", *J. Lightwave Technol.*, **30**(8), 1066-1072.

CC